Bull. Chem. Soc. Ethiop. **2023**, 37(5), 1123-1131.
DOI: https://dx.doi.org/10.4314/bcse.v37i5.5

ISSN 1011-3924
Printed in Ethiopia
Online ISSN 1726-801X

SYNTHESIS AND CHARACTERIZATION OF TERNARY COMPOSITE g-C_3N_4-WO_3/rGO FOR PHOTOCATALYTIC ACTIVITY IN DEGRADATION OF METHYLENE BLUE

Zainab Waheed[1], Sadia Ghazanfar[1], Muhamamd Usman[2], Hafiz Muhammad Asif[1], Muhammad Tariq[1*], Khalid Mahmood[1], Ali Haider[3] and Muhammad Sirajuddin[4]

[1]Institute of Chemical Sciences, Bahauddin Zakariya University, 60800, Multan, Pakistan
[2]Institute of Biomedical Materials and Engineering, College of Materials Science and Engineering, Qingdao University, 308 Ningxia Road, Qingdao, Shangdong 266071, China
[3]Department of Chemistry, Quaid-e-Azam University Islamabad, Pakistan
[4]Department of Chemistry, University of Science & Technology, 28100 Bannu, Pakistan

(Received January 2, 2023; Revised March 24, 2023; Accepted March 28, 2023)

ABSTRACT. In the present research work, ternary composite g-C_3N_4-WO_3/rGO was prepared by using ultrasonic assisted wet impregnation procedure. The prepared ternary composite was characterized by using FT-IR, powder XRD, SEM, and EDX techniques. FTIR studies confirmed the presence of characteristic bonds of the representative components in the composite by showing their characteristic peaks. The XRD pattern of ternary composite g-C_3N_4-WO_3/rGO showed the presence of peaks responsible for monoclinic phase of pure tungsten oxide (WO_3) and the characteristic peaks of graphitic C_3N_4 and GO. SEM studies of g-C_3N_4-WO_3/rGO revealed the presence of randomly dispersed tungsten oxide particles in between agglomerated 2-D layers of carbon nitride and GO sheets. EDX data confirmed the phase purity in the form of elemental composition of the prepared composite and further provided At wt% of each element in the composite. Photocatalytic activity of the synthesized composite was evaluated by performing photocatalytic degradation test of methylene blue (MB). The rate of degradation was measured by using Shimadzu UV-1800 UV-Vis Spectrophotometer by recording the decreasing concentration of dye in terms of their absorbance values. The results exhibited that g-C_3N_4-WO_3/rGO showed better degradation efficiency in 180 min.

KEY WORDS: Impregnation, Composite, Photocatalyst, Degradation, Methylene blue

INTRODUCTION

Fast industrialization, new growth processes and increasing population have been continuously deteriorated global environment [1, 2]. The organic pollutants from various sources like industrial, agricultural, chemical spills have been polluting water dangerously which is becoming threat for human as well as aquatic organisms [3]. The organic dyes have been used extensively in various industries like textile, leather, paper and pulp, etc. and are being discharged in industrial effluents. Various studies have been conducted on degradation of these organic dyes by photocatalyst [4-9], but there is lot of scope to find out an ultimate solution.

The design and development of photocatalyst worked under visible light for degradation of organic pollutant has been an interesting and challenging research field now a day [10-12]. WO_3 is a semiconductor photocatalyst with band gap of 2.8 eV has got attention during the last few years due to its visible light harvesting ability but it has limitations of quick electron-hole recombination, slow charge transfer rate, etc. [13, 14]. Various types of processes like doping with metals, coupling with some other materials have been reported to enhance photodegradation activity of WO_3 [15-18]. WO_3/rGO composite has been reported with enhance photocatalytic activity because of large surface area, fast charge transfer and separation of carriers, good thermal conductivity properties of 2-D, single layered graphene [19, 20]. In the present study, we have coupled three components, WO_3, rGO and g-C_3N_4 to form ternary composite (g-C_3N_4-WO_3/rGO)

*Corresponding author. E-mail: mtnazir@yahoo.com

with expectation of improved degradation efficiency due to interaction of three multifunctional components which may lead to formation of electron-hole puddle and fast charge transfer processes.

EXPERIMENTAL

Graphitic C_3N_4 synthesis

The graphitic-C_3N_4 was freshly prepared by using already reported procedure [21]. For reproduction, the method is given as briefly, 4.0 g melamine was taken in a corundum crucible and heated in a furnace at 500 °C for 2 hours initially and at 520 °C for another 2 hours. Then it was cooled to room temperature, finally yellow color product was obtained and ground to fine powder.

GO synthesis

The modified Hummer's method [22] was used to prepare GO. The method is briefly described as, 1.0 g of crystalline graphite powder was taken in a 500 mL beaker and then 45 mL of conc. sulfuric acid was added. The reaction mixture was kept on stirring for 12 hours. After this, the reaction mixture was cooled by adding ice cold water to about 12 °C. Then 3.0 g potassium permanganate was added slowly and the temperature was slowly increased to 35 °C while stirring for two hours. The mixture was put in ultrasonic bath for sonication for half an hour. The obtained suspension was put on stirring again and 100 mL deionized water was added slowly. In the final step H_2O_2 (6%) was put into the above suspension until zero effervescence. Finally, the mixture was put in centrifugation to get the final product which was then washed with dil. HCl several times and deionized water to remove any left impurities. The ultimate product was dried in an oven at 70 °C overnight.

WO_3 synthesis

Hydrothermal method was used to prepare WO_3 nanoparticles [23]. $Na_2WO_4.2H_2O$ (1.005 g) and NaCl (0.931 g) were dissolved in 30 mL deionized water and stirred for 15 min. The pH was maintained at 2 by addition of 3 M HCl. The solution was stirred further for three hours. Then solution was taken into 100 mL autoclave (Teflon-lined stainless) and placed in oven at temperature of 180 °C for 24 hours. The resultant precipitated product was collected by centrifugation and washed with deionized water and ethanol several times. The final washed product was dried at 60 °C in drying oven. The dried product was calcined at 450 °C for 4 hours to remove any impurities.

Preparation of g-C_3N_4-WO_3

g-C_3N_4-WO_3 was prepared by ultrasonic assisted wet impregnation method [22]. 0.3 g WO_3 (30 wt %) was dissolved into a mixture of ethanol and water (1:1) and put on stirring for 3 hours. Then 0.7 g g-C_3N_4 (70 wt %) was mixed into the solution. The resultant mixture was kept on stirring and heating until dryness. The product was placed in an oven at 70 °C for complete drying. The final product was obtained by calcination at 400 °C for one hour.

Preparation of g-C_3N_4-WO_3/rGO

Ternary composite g-C_3N_4-WO_3/rGO was synthesized using wet impregnation method [22]. First of all, an appropriate weight of graphene oxide solution was made by dissolving GO powder in 40 mL of a mixture of solvents (ethanol and deionized water in 1:1 ratio) and then sonicated for 1 hour. Then 0.3 g of WO_3 (30 wt %) was put into the above solution and stirred for 2 hours. Lastly 0.7 g g-C_3N_4 (70 wt %) was added and the whole mixture was stirred and heated slowly

until the evaporation of all solvent. The resultant product was placed in an oven at 70 °C for drying and then calcined at 400 °C for 1 hour to get final ternary composite product.

Photocatalytic application in degradation of MB dye

The g-C_3N_4-WO_3/rGO photocatalytic application as visible light driven photocatalyst was investigated in degradation of methylene blue (MB). 200 W bulb was used as source of visible light. 10 ppm initial dye concentration was used. The Pyrex reactor was 10 cm apart from the source of visible light. The dye degradation was observed by using UV- visible spectrophotometer (Shimadzu UV-1800) measuring change in absorbance (λ_{max}) value of dye. The sample aliquot was taken at a regular interval of time and degradation rate was recorded at λ_{max} of 664 nm for MB.

First of all blank experiment without using photocatalyst was performed in which 10 ppm dye solution was placed under 200 W bulb (visible light source) and then absorbance was recorded. After blank experiment, 0.05 g photocatalyst was added into 10 ppm dye solution. The resultant solution was placed in dark for one hour under stirring so that an absorption-desorption equilibrium is achieved. Then reactor was illuminated using 200 W visible light source for a xenon lamp and allowed for degradation process within dye solution having photocatalyst. After a regular interval of time, 4 mL sample solution was taken out of the reactor, centrifuged at 4500 rpm for about 5 min to separate catalyst and then absorbance was recorded in visible range of 800-400 nm.

RESULTS AND DISCUSSION

FT-IR studies

In FT-IR spectrum of g-C_3N_4, the main characteristics out of phase bending vibration peak appeared at 807.15 cm^{-1} which represent breathing mode of triazine units. The C-N fully condensed (C-N(-C)-C) and partially condensed (C-N-H) peaks were appeared at 1206.39 cm^{-1}, 1242.07 cm^{-1} and 1318.25 cm^{-1}, respectively. While C=N stretching vibration band appeared at 1664.45 cm^{-1}. The N-H and OH broad peaks were appeared at 3039.60 cm^{-1} and 3338.55 cm^{-1}, respectively. In FT-IR spectrum of GO, the main characteristics peak due to C-O stretching vibration appeared at 1018 cm^{-1}. The stretching vibration of tertiary C-OH group appeared at 1348 cm^{-1}. The peak appeared at 1560 cm^{-1} is assigned to unoxidized C=C bonds. The –OH stretching broad band due to absorbed water molecule appeared at 3360.73 cm^{-1}.

In the FT-IR spectrum of pure WO_3 the two main characteristics peaks due to O-W-O stretching vibration were appeared at 731.94 cm^{-1} and 815.83 cm^{-1}. A broad band at 3450 cm^{-1} was assigned to OH stretching vibration band of water molecule absorbed on surface of WO_3.

By comparing FT-IR result of GO with WO_3/rGO, it is noted that characteristic peak of GO disappeared in hybrid composite which may be due to relatively lower concentration of GO and its reduction to rGO. The binary composite g-C_3N_4-WO_3 FT-IR results showed that all characteristics peaks of g-C_3N_4 e.g. 807.15, 1235.32, 1244.00 and 1530.60 cm^{-1} appeared but the peak of WO_3 not appeared which may be due to relatively lower weight of WO_3 and coupling of graphitic carbon nitride with tungsten oxide.

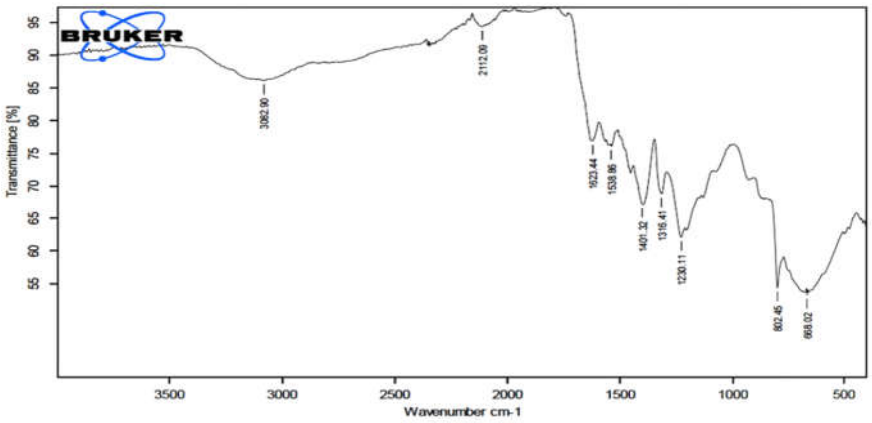

Figure 1. FT-IR Spectrum of g-C_3N_4-WO_3/rGO ternary composite.

In the FT-IR spectrum of ternary composite (g-C_3N_4-WO_3/rGO) as represented in Figure 1, it has been observed that a peak appeared at 802.45 cm^{-1}represent triazine units. This band does not change after coupling however other characteristics peaks appeared at 1230.11 and 1316.14 cm^{-1} showed a little change in wavenumber indicating coupling of three components. The broad band appeared at 3382.90 cm^{-1} has been assigned to O-H stretching band for water molecule adsorbed on the surface. The GO and WO_3 characteristics peaks were disappeared in the spectrum which may be due to reduction of GO to rGO and interfacial interaction with g-C_3N_4.

XRD studies

The XRD patterns of pure, binary and ternary composite of tungsten oxide are represented in Figure 2. The peak pattern of pure WO_3 at various θ values exhibit its crystalline nature of monoclinic phase (JCPDS 72-1465) with the sharp peak at 2θ = 23°. The binary g-C_3N_4-WO_3 composite and ternary g-C_3N_4-WO_3/rGO composite XRD peak pattern are similar except a sharp and strongest peak with high intensity at 2 θ = 27.20° with 002 plane which is appeared due to coupling interaction of WO_3/rGO with g-C_3N_4.

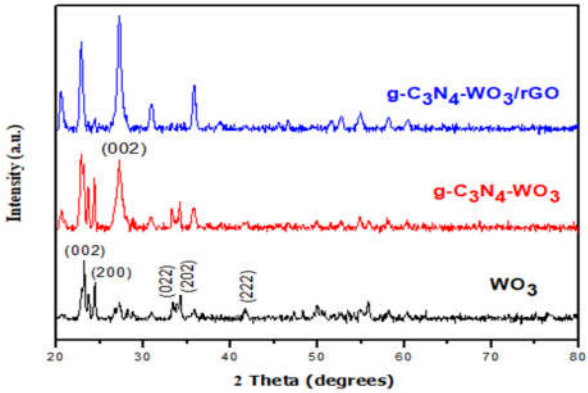

Figure 2. Powder XRD of pure, binary and ternary composite of tungsten oxide.

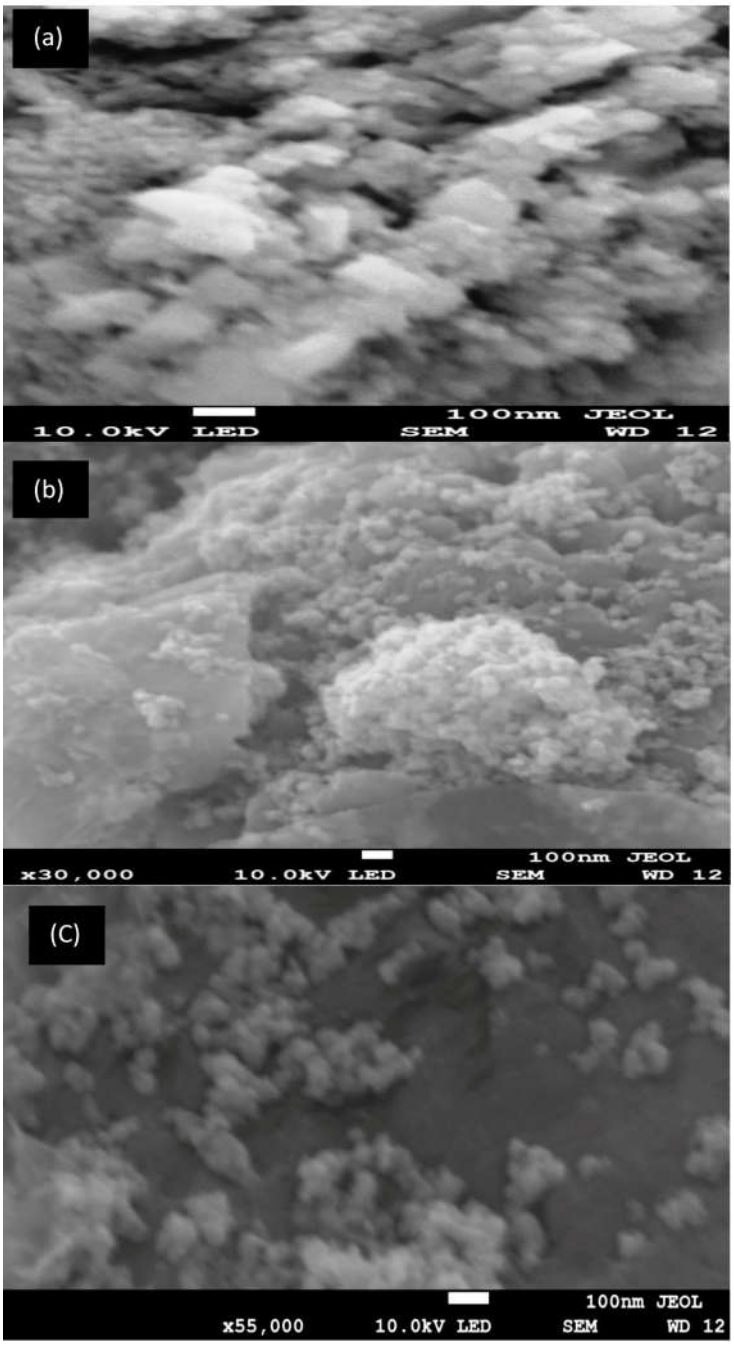

Figure 3. Scanning electron microscopy images (a) Pure WO_3, (b) g-C_3N_4-WO_3 and (c) g-C_3N_4-WO_3/rGO.

SEM analysis

The morphology and structural characteristics of pure WO_3, g-C_3N_4/WO_3 and g-C_3N_4-WO_3/rGO were characterized by SEM analysis given in Figure 3a-c. The bare WO_3 consists of agglomerated and accumulated plate like morphology with particle size of 150 nm as sown in Figure 3a. The Figure 3b represents the anchoring of these agglomerated and accumulated plates like WO_3 particles on layered sheet of carbon nitride and calculated particle size is 135 nm. The layer surface of g-C_3N_4 was covered by high density bare agglomerated and accumulated plate like WO_3 nanoparticles. The anchoring of these agglomerated and accumulated WO_3 particles on sheet like g-C_3N_4 could results decrease in size. Figure 3c showed the randomly dispersion of agglomerated WO_3 nanoparticles on the layer of g-C_3N_4 and sheet of rGO with average calculated particle size of 100 nm. When WO_3/g-C_3N_4 is enveloped on 2-dimensional layered GO sheet, the further decrease in size has been observed which could be due to stacked and interconnected heterostructure formation.

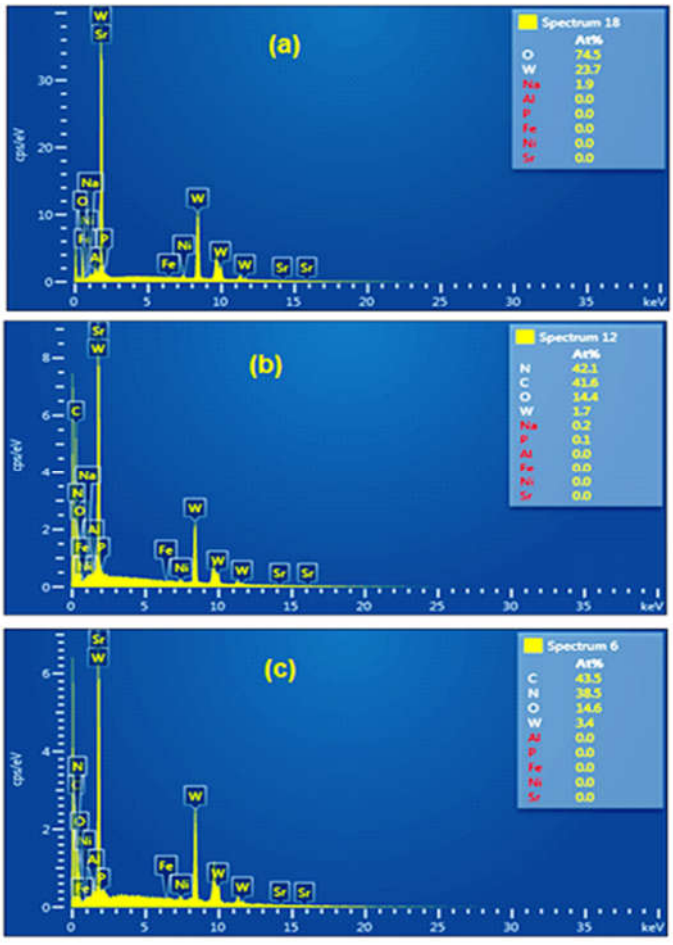

Figure 4. EDX spectra (a) Pure WO_3, (b) g-C_3N_4-WO_3 and (c) g-C_3N_4-WO_3/rGO.

EDX (Energy dispersive X-ray) analysis

EDX was used to find out elemental composition of pure WO_3, binary composite g-C_3N_4-WO_3 and ternary composite g-C_3N_4-WO_3/rGO and spectra are represented in Figure 4a-c. The elemental composition of pure WO_3 is represented in Figure 4a which showed 23.7 At % of W and 74.5 At % of oxygen. This shows that pure WO_3 is formed.

The elemental composition spectrum of binary composite g-C_3N_4-WO_3 is represented in Figure 4b. The Figure 4b showed that W (tungsten) is present as prominent element. The atomic percentage of other elements C, N and O are represent in inset Figure 4b. The overall At % of W, C, N and O confirmed formation of g-C_3N_4-WO_3 binary composite.

The elemental composition spectrum of g-C_3N_4-WO_3/rGO ternary composite is represented in Figure 4c which showed prominent existence of W along with other concerned elements like O, C and N. The atomic percentage (At %) of elements in the ternary composites was given in inset in the Figure 4c. The carbon atomic percentage was contributed from g-C_3N_4 while oxygen atom was contributed from WO_3 and a small percentage from rGO in the ternary composite.

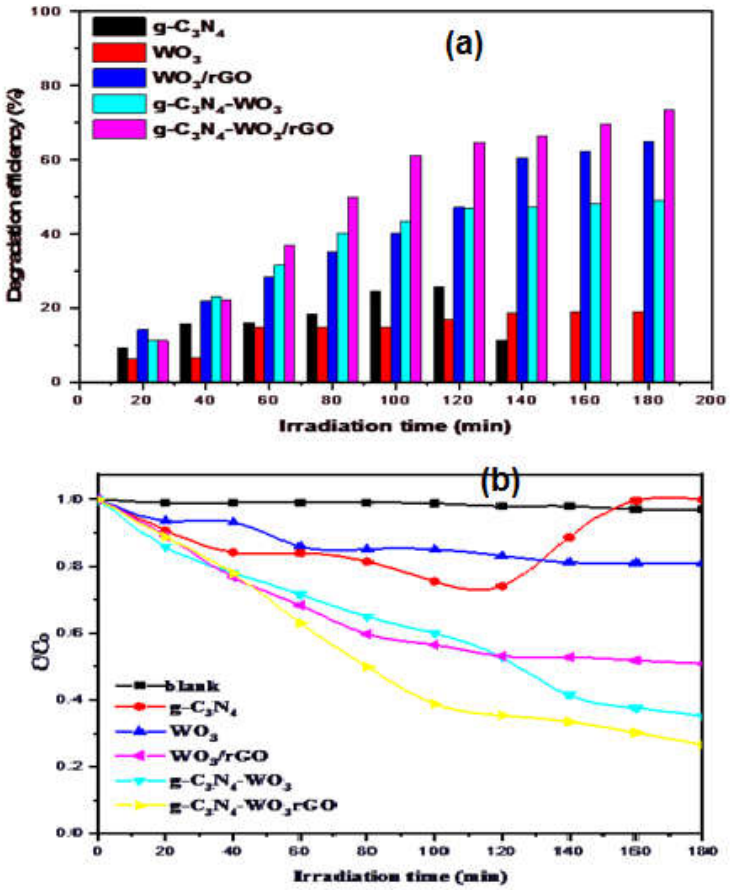

Figure 5. Degradation rate (a) and visible light driven photogradation of methylene blue (b) using g-C_3N_4, WO_3, WO_3/rGO, g-C_3N_4-WO_3 and g-C_3N_4-WO_3/rGO.

Photocatalytic degradation application

The degradation property of ternary composite g-C_3N_4-WO_3/rGO along with all building precursors like WO_3, g-C_3N_4, WO_3/rGO, g-C_3N_4-WO_3 was performed with methylene blue dye (MB). The results are presented in Figure 5. The blank test with methylene blue dye was performed first which result no change in absorption indicating stability of dye. The pure WO_3 exhibited only 19% degradation efficiency. This may be due poor absorbance activity and fast recombination of electron hole pair. The binary composite g-C_3N_4-WO_3 and WO_3/rGO showed comparatively better degradation efficiency of 64% and 49%, respectively. While ternary composite g-C_3N_4-WO_3/rGO exhibited better degradation efficiency of 76% which may be due to more electron acceptor ability absorbance of UV light and large surface area. The increase in degradation efficiency is due to coupled interaction of three components.

CONCLUSION

Ternary composite of g-C_3N_4-WO_3/rGO was successfully prepared by ultrasonic wet impregnation method and its photocatalytic activity in degradation of methylene blue was evaluated. The results showed 76% degradation efficiency. For comparison, pue WO_3 and binary composite g-C_3N_4-WO_3 were also prepared and their photocatalytic activity was compared. The formation of pue WO_3, binary composite g-C_3N_4-WO_3 and ternary composite g-C_3N_4-WO_3/rGO was confirmed by FT-IR, XRD, SEM and EDX analysis. The ternary composite exhibited better photo-degradation activity than both pure and binary composite. This may be due to coupled effect of three components which resulted in enhance charge transfer process, smooth transfer of electrons and inhibit fast electron-holes recombination.

ACKNOWLEDGEMENTS

The authors are thankful to Bahauddin Zakariya University Multan, Pakistan for financial support during the research work.

REFERENCES

1. Marques Junior, A.N.; Panetto, D.P.; Lamego, F.; Nepomuceno, F.O.; Monna, F.; Losno, R.; Guillon, R. Tracking atmospheric dispersion of metals in Rio de Janeiro Metropolitan region (Brazil) with epiphytes as bioindicators. *Annals Braz. Acad. Sci.* **2018,** 90, 2991-3005.
2. Balaji, S.; Kalaivani, T.; Rajasekaran, C.; Shalini, M.; Vinodhini, S.; Sunitha Priyadharshini, S.; Vidya, A.G. Removal of heavy metals from tannery effluents of Ambur industrial area, Tamilnadu by Arthrospira (Spirulina) platensis. *Environ. Monit. Assess.* **2015**, 187, 1-10.
3. Neelavannan, M.; Revathi, M.; Basha, C.A. Photocatalytic and electrochemical combined treatment of textile wash water. *J. Hazard. Mater.* **2007**, 149, 371-378.
4. Anjaneyulu, Y.; Sreedhara Chary, N.; Samuel Suman Raj, D. Decolourization of industrial effluents–available methods and emerging technologies–a review. *Rev. Environ. Sci.* **2005**, 4, 245-273.
5. Liao, G.; Chen, S.; Quan, X.; Yu, H.; Zhao, H. Graphene oxide modified gC_3N_4 hybrid with enhanced photocatalytic capability under visible light irradiation. *J. Mater. Chem.* **2012**, 22, 2721-2726.
6. Han, F.; Kambala, V.S.R.; Srinivasan, M.; Rajarathnam, D.; Naidu, R. Tailored titanium dioxide photocatalysts for the degradation of organic dyes in wastewater treatment. *Appl. Catal. A: Gen.* **2009**, 359, 25-40.

7. Akhundi, A.; Habibi-Yangjeh. A. Ternary g-C_3N_4/ZnO/AgCl nanocomposites: synergistic collaboration on visible-light-driven activity in photodegradation of an organic pollutant. *Appl. Surf. Sci.* **2015**, 358, 261-269.
8. Chang, Y.; Liu, X.; Cai, A.; Xing, S.; Ma, Z. Glycine-assisted synthesis of mesoporous TiO_2 nanostructures with improved photocatalytic activity. *Ceram. Int.* **2014**, 14765-14768.
9. Sharma, M.; Singh, J.; Basu, S. Efficient metal ion adsorption and photodegradation of Rhodamine-B by hierarchical porous Fe-Ni@ SiO2 monolith. *Microchem. J.* **2019**, 145, 708-717.
10. Singh, J.; Ankita, A.; Soumen, B. Synthesis of coral like WO_3/g-C_3N_4 nanocomposites for the removal of hazardous dyes under visible light. *J. Alloys Compd.* **2019**, 808, 151734.
11. Cui, L.; Ding, X.; Wang, Y.; Shi, H.; Huang, L.; Zuo, Y.; Kang, S. Facile preparation of Z-scheme WO_3/g-C_3N_4 composite photocatalyst with enhanced photocatalytic performance under visible light. *Appl. Surf. Sci*. **2017**, 391, 202-210.
12. Chai, B.; Liu, C.; Yan, J.; Ren, Z.; Wang, Z.J. In-situ synthesis of WO_3 nanoplates anchored on g-C_3N_4 Z-scheme photocatalysts for significantly enhanced photocatalytic activity. *Appl. Surf. Sci*. **2018**, 448, 1-8.
13. Chen, X.; Zhou, B.; Yang, S.; Wu, H.; Wu, Y.; Wu, L.; Xiong, X. In situ construction of an SnO_2/gC_3N_4 heterojunction for enhanced visible-light photocatalytic activity. *RSC Adv.* **2015**, 84, 68963.
14. Aslam, I.; Cao, C.; Tanveer, M.; Khan, W.S.; Tahir, M.; Abid, M.; Mahmood, N. The synergistic effect between WO_3 and gC_3N_4 towards efficient visible-light-driven photocatalytic performance. *New J. Chem*. **2014**, 38, 5462-5469.
15. Chen, S.; Hu, Y.; Meng, S.; Fu, X. Study on the separation mechanisms of photogenerated electrons and holes for composite photocatalysts g-C_3N_4-WO_3. *Appl. Catal. B* **2014**, 150, 564-573.
16. Zhu, W.; Sun, F.; Goei, R.; Zhou, Y. Construction of WO_3–gC_3N_4 composites as efficient photocatalysts for pharmaceutical degradation under visible light. *Catal. Sci. Technol*. **2017**, 7, 2591-2600.
17. Chen, S.; Hu, Y.; Jiang, X.; Meng, S.; Fu, X. Fabrication and characterization of novel Z-scheme photocatalyst WO_3/g-C_3N_4 with high efficient visible light photocatalytic activity. *Mater. Chem. Phys,* **2015**, 149, 512-521.
18. Huang, L.; Xu, H.; Li, Y.; Li, H.; Cheng, X.; Xia, J.; Cai, G. Visible-light-induced WO_3/gC_3N_4 composites with enhanced photocatalytic activity. *Dalton Trans*. **2013**, 42, 8606-8616.
19. Abd Elhakim, A.; El-Kemary, M.; Ibrahim, M.M.; El-Mehasseb, I.M.; El-Sheshtawy, H.S. Direct Z-scheme of WO_3/GO decorated with silver nanoparticles for synergetic adsorption and photocatalytic activity for organic and inorganic water pollutants removal. *Appl. Surf. Sci.* **2021**, 564, 150410.
20. Jeevitha, G.; Abhinayaa, R.; Mangalaraj, D.; Ponpandian, N. Tungsten oxide-graphene oxide (WO_3-GO) nanocomposite as an efficient photocatalyst, antibacterial and anticancer agent. *J. Phys. Chem. Solids* **2018**, 116, 137-147.
21. Katsumata, H.; Tachi, Y.; Suzuki, T.; Kaneco, S. Z-scheme photocatalytic hydrogen production over WO_3/gC_3N_4 composite photocatalysts. *RSC Adv.* **2014**, 4, 21405-21409.
22. Zainab, W.; Sadia, G.; Muhammad, U.; Khalid, M.; Ajaz, H.; Sirajuddin, M.; Tariq, M. Synthesis and characterization of ternary composite g-C_3N_4-MoO_3/rGO for photocatalytic activity. *Mediterr. J. Chem.* **2023**, 13, 50-58.
23. Zhao, J.; Ji, Z.; Shen, X.; Zhou, H.; Ma, L. Facile synthesis of WO_3 nanorods/g-C_3N_4 composites with enhanced photocatalytic activity. *Ceram. Int.* **2015**, 41, 5600-5606.